

# A Low Complexity Coherent 16×400 Gbit/s 4SC-16QAM DSCM system with Precise Transceiver IQ Skew Compensation and Simplified Equalization

Wei Wang<sup>1,2</sup>, Dongdong Zou<sup>1,2</sup>, Zhenpeng Wu<sup>1,2</sup>, Xingwen Yi<sup>1,2</sup>, Wei Sun<sup>3</sup>, Fan Li<sup>1,2,\*</sup>, and Zhaohui Li<sup>1,2</sup>

<sup>1</sup>School of Electronics and Information Technology, Guangdong Provincial Key Laboratory of Optoelectronic Information Processing Chips and Systems, Sun Yat-Sen University, Guangzhou 510275, China

<sup>2</sup>Southern Marine Science and Engineering Guangdong Laboratory (Zhuhai), Zhuhai, China

<sup>3</sup>R & D Department, Hengtong Optic-electric Co., Ltd., Suzhou 215200, China

Email: [lijan39@mail.sysu.edu.cn](mailto:lijan39@mail.sysu.edu.cn)

**Abstract:** A low complexity coherent 16×400 Gbit/s datacenter interconnect with 50Gbaud 4SC-16QAM DSCM signal is experimentally demonstrated, enabled by a novel low complexity transceiver IQ skew estimation method and simplified equalizer embedded phase tracking. © 2024 The Author(s)

## 1. Introduction

Digital subcarrier multiplexing (DSCM) technique has been regarded as an attractive solution in power consumption sensitive datacenter interconnect (DCI), which exhibits the potential in the simplification of the dispersion compensation [1, 2]. However, compared to the conventional single carrier system, the DSCM signal is more sensitive to the transceiver IQ skew. The subcarriers will suffer severe interference from symmetrical frequency subcarriers in the presence of transceiver IQ skew, especially for the subcarriers located at high frequency, causing seriously performance degradation [3]. Multiple-in multiple-out (MIMO) equalizer is an effective method to address IQ skew impairments [4]. Different from the single-carrier system, an 8×8 real-value MIMO equalizer is required for a symmetric subcarrier pair in DSCM systems, resulting in high computational complexity [5, 6].

In this paper, we propose a novel low-complexity transceiver IQ skew estimation method based on specially designed training signal to compensate both the Tx-skew and Rx-skew for DSCM systems to avoid complicated 8×8 real-value MIMO equalizer. Besides, to further reduce the computational complexity of the Rx-DSP, a simplified equalizer structure embedded a 1-tap phase factor is also proposed, which cascades a 1-tap 2×2 MIMO and two N-tap single-in single-out (SISO) equalizers. The proposed method is proved in 50Gbaud 4SC-16QAM DSCM WDM system with 16 channels. The results show that about 6dB OSNR gain can be obtained at the HD-FEC threshold after transceiver IQ skew compensation. And there is almost no performance penalty of the proposed simplified equalizer compared to the conventional CMMA combined blind phase search (BPS) method. According to the results, the proposed low complexity coherent DSCM scheme is a promising solution for DCI applications.

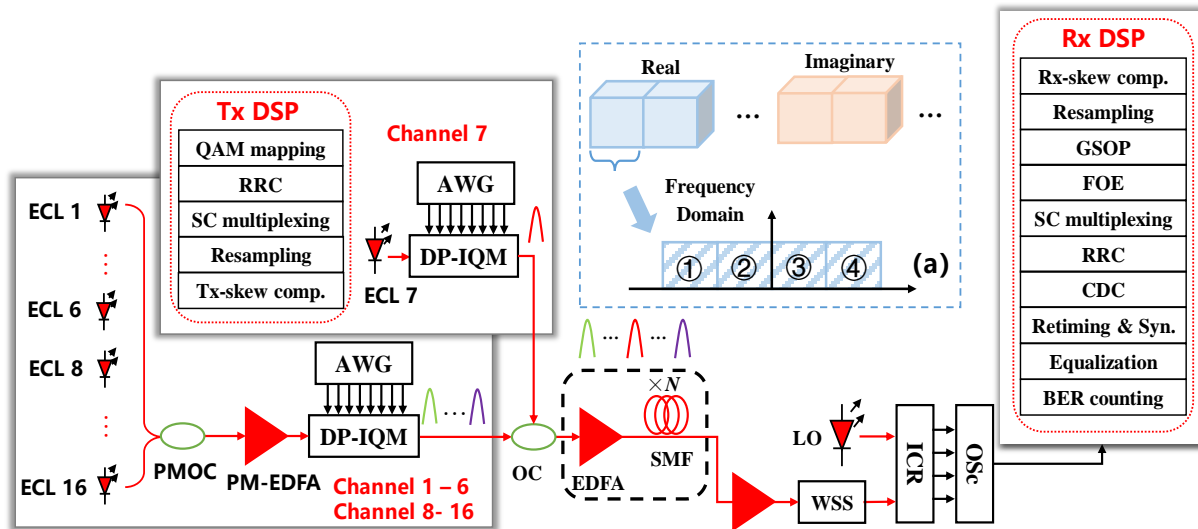


Fig. 1. Experimental setup and DSP flow. (a) Training signal structure.

## 2. Operation Principle

Figure 1(a) gives the structure of the specially designed training signal in the single-polarization case. The first half of the training sequence is real, while the second half is imaginary, which is transmitted individually in I and Q channels at different time periods. And the signal exhibits the feature of being composed of four identical blocks in the frequency domain. The signals with Tx-skew are denoted as  $s_{Tx}^I$  and  $s_{Tx}^Q$ , where the superscript means the signal transmitted in I/Q channel at the transmitter. And denoting the real and imaginary parts of the received signal with Rx-skew as  $s_{Rx-I}^I$  and  $s_{Rx-Q}^I$  respectively. By performing correlation operation between adjacent frequency blocks of the training signal in frequency domain, we can obtain:

$$\begin{aligned} CrrS_{Rx-I}^I &= \sum S_{Rx-I}^I(k) \cdot S_{Rx-I}^{I*}(k+N_d) \\ &\approx \sum \frac{1}{4} e^{-j\phi_{Rx}^I N_d} \cdot \left[ S^I(k-k_1) \cdot S^I(k-k_1+N_d) \cdot e^{-j\phi_{Tx}^I N_d} + S^I(k+k_1) \cdot S^I(k+k_1+N_d) \cdot e^{-j\phi_{Tx}^I N_d} \right] \end{aligned} \quad (1)$$

where  $N_d$  is the size of each block,  $\phi_{Tx}^I = -2\pi\tau_{Tx}^I / N$ ,  $\phi_{Rx}^I = -2\pi\tau_{Rx}^I / N$  ( $\tau_{Tx/Rx}^{I/Q}$ : time delay in I/Q channel at Tx/Rx), and  $k_1$  is the frequency offset. Similaly,  $CrrS_{Rx-Q}^I$  can be calculated by the correlation operation of  $S_{Rx-Q}^I(k)$ . The Rx-skew can be calculated by:

$$\tau_{Rx}^Q - \tau_{Rx}^I = \frac{N}{2\pi N_d} \left[ \text{angle}(CrrS_{Rx-Q}^I) - \text{angle}(CrrS_{Rx-I}^I) \right] \quad (2)$$

By together utilizing the second half of the sequence, the Tx-skew can also be obtained by:

$$\tau_{Tx}^Q - \tau_{Tx}^I = \frac{N}{2\pi N_d} \left[ \text{angle}(CrrS_{Rx-Q}^Q) - \text{angle}(CrrS_{Rx-I}^I) \right] \quad (3)$$

## 3. Experimental setup and results

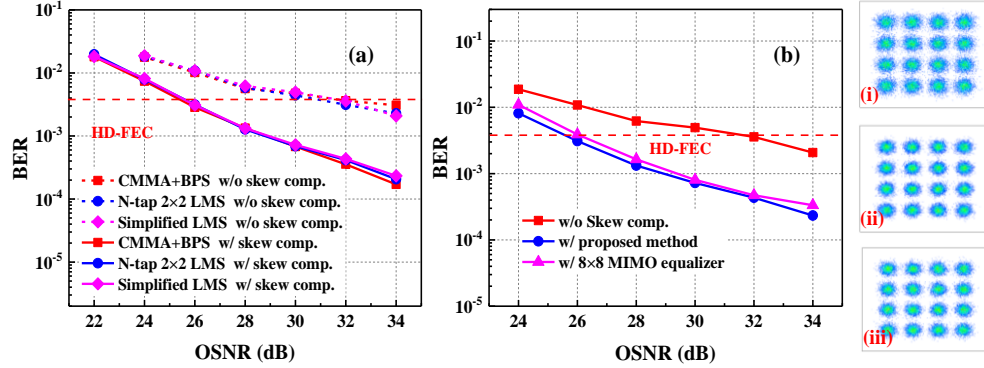


Fig. 2. BER curves with (a) three equalizers and (b) different skew compensation methods in single wavelength OBTB transmission.

Figure 1 shows the experimental setup of 16×400 Gbit/s 4SC-16QAM DSCM WDM system. At the transmitter, 16 tunable external cavity lasers (ECLs) with 75GHz grid are used as the optical carriers for the WDM transmission. The output power and linewidth of each optical carrier are 16dBm and less than 100kHz respectively. In our experiment, one optical carrier is input into a dual-polarization IQ modulator (DP-IQM) to generate the tested signal, while other 15 carriers are coupled and then injected into another DP-IQM to be used as the untested channels. To compensate the power difference between the tested channel and other coupled 15 channels, a polarization maintaining Erbium-doped fiber amplifier (PM-EDFA) is used for the coupled carriers. Then, the output signals from the two modulators are coupled together and injected into several cascaded fiber spans. Each span contains an EDFA and 80km single mode fiber (SMF). After fiber transmission, another EDFA is used to compensate the power loss. At the receiver, the tested wavelength is filtered out by the programmable wavelength selective switch (WSS). The selected signal together with the local oscillator (LO) is input into a finisar 40-G class integrated coherent receiver (ICR) for coherent detection. And the detected signals are captured by a Lecory oscilloscope (Osc) with 80GSa/s sampling rate. The signal generation and processing is achieved in the offline matlab, and the digital signal processing (DSP) algorithms are given in Fig. 1. In the calibration phase, a specially designed training signal is used

to estimate the transceiver IQ skew. Based on the estimated skew values, the Tx-skew is calibrated before loading to the DP-IQM. As for the Rx-DSP, Rx-skew compensation is done first. And the following DSP algorithms include resampling, Gram-Schmidt orthogonalization procedure (GSOP), pilot tone based frequency offset compensation, SC demultiplexing, root raised cosine (RRC) filter, CDC, retiming, synchronization, equalization and BER counting.

To evaluate the effectiveness of the proposed transceiver IQ skew compensation and simplified equalizer, the BER performance versus OSNR in single wavelength OBTB transmission is measured and shown in Fig. 2(a). The performance based on the simplified equalizer is compared to that using conventional 2×2 MIMO CMMA with BPS, and N-tap 2×2 MIMO LMS equalizer combined with 1-tap phase factor. The proposed simplified equalizer shows the similar performance to the other two schemes as shown in Fig. 2(a). After transceiver IQ skew compensation, about 6dB OSNR gain can be observed at the HD-FEC threshold. Fig. 2(b) also gives the BER performance utilizing 8×8 real-value MIMO equalizer to compensate the transceiver IQ skew. It can be seen that the proposed method shows the similar performance to the 8×8 real-value MIMO, while operating in a lower complexity manner. Fig. 3(a) shows the measured BER of the 7<sup>th</sup> channel under different OSNRs in WDM transmission. According to the results, there is almost no OSNR penalty in WDM transmission compared to the corresponding single channel transmission in OBTB. The performance in fiber transmission is also investigated. Fig. 3(b) gives the BER performance of the 7<sup>th</sup> channel under different transmission distances with three equalization schemes, and the total launch power of combined WDM channels is about 12dBm. When the transmission distance less than 560km, the performance utilizing these three equalization schemes is almost the same. However, the performance with the proposed simplified equalizer is inferior to the other two schemes when fiber length is longer than 560km, since the 1-tap MIMO fails to address the influence of polarization mode dispersion (PMD) well. The BER performance of all 16 channels over 640km SMF transmission with the proposed simplified equalizer and transceiver IQ skew compensation is given in Fig. 3(c). All the measured BER can be below the SD-FEC threshold after 640km SMF transmission. And the optical spectra of 16-channel WDM signals in OBTB is inserted in Fig. 3(c).

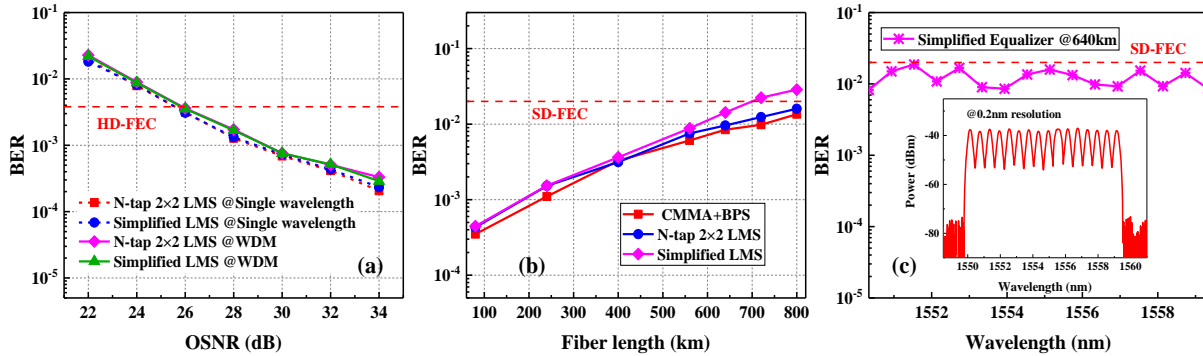


Fig. 3. (a) BER versus OSNR in OBTB, (b) BER versus fiber length and (c) measured BER of all 16 channels in WDM transmission.

#### 4. Conclusion

The demonstration of 16×400 Gbit/s 4SC-16QAM DSCM WDM transmission with transceiver IQ skew compensation and simplified equalizer method is experimentally achieved. A specially designed training signal is used to realize precise and low complexity skew estimation, and about 6dB OSNR gain can be obtained at the HD-FEC threshold after skew compensation. Besides, there is almost no performance penalty by utilizing the simplified equalizer compared to the conventional equalization and phase noise compensation method. Therefore, the proposed low complexity coherent DSCM scheme shows the potential for application in DCI.

#### 5. Acknowledge

This work is partly supported by the National Key R&D Program of China (2021YFB2900702); Guangdong Basic and Applied Basic Research Foundation (2023B1515020003); National Natural Science Foundation of China (62271517); Open Fund of IPOC (BUPT) (IPOC2020A010).

#### 6. References

- [1] H. Sun, et al., JLT, 38(17), 4744-4756, 2020.
- [2] D. Krause, et al., OFC 2017, Th1D.1.
- [3] T. Duthel, et al., JLT, Early access, 2016.
- [4] E. P. da Silva, et al., JLT, 34(15), 3577-3586, 2016.
- [5] W. Tong, et al., PJ, 15(4), 1-8, 2023.
- [6] L. Fan, JLT, 41(19), 6187-6198, 2023.